Наносистеми, наноматеріали, нанотехнології
Nanosistemi, Nanomateriali, Nanotehnologii
2022, т. 20, № 3, сс. 647–655

PACS numbers: 61.05.cp, 61.43.Gt, 68.37.-d, 68.65.-k, 77.55.hf, 78.67.Rb, 81.05.Rm

ZnO/SiC/Porous-Si/Si Heterostructure: Obtaining and Properties

V. V. Kidalov[1], V. P. Kladko[2], A. F. Dyadenchuk[1], O. I. Gudymenko[2], V. A. Baturin[3], A. Yu. Karpenko[3], and V. V. Kidalov[4]

[1]*Dmytro Motornyi Tavria State Agrotechnological University,*
18, B. Khmelnytsky Ave.,
UA-72312 Melitopol, Ukraine
[2]*V. E. Lashkaryov Institute of Semiconductor Physics, N.A.S. of Ukraine,*
41, Nauka Ave.,
UA-03028 Kyiv, Ukraine
[3]*Institute of Applied Physics, N.A.S. of Ukraine,*
58, Petropavlivska Str.,
UA-40000 Sumy, Ukraine
[4]*Berdyansk State Pedagogical University,*
4, Schmidt Str.,
UA-71100 Berdyansk, Ukraine

The content of this work demonstrates the zinc-oxide (ZnO) films' synthesis by means of the HF magnetron sputtering of a zinc target on a silicon substrate using the buffer layers of SiC and porous Si. The synthesis is consisted of three stages: obtaining a mesoporous Si(111) surface by electrochemical etching, SiC films' deposition on porous silicon substrates by the substitution method, and ZnO films' synthesis using the high-frequency magnetron sputtering. The zinc-oxide film thickness is of $\cong 1$ μm. A microscopic cross-section image of the ZnO film demonstrates its columnar microstructure. The films are in the form of tightly packed (agglomerated) nanograins (of 100–150 nm in size). According to the XRD-measurement results, the ZnO films are oriented along the main texture direction [0001]. The study of the formed-structure surface properties indicates the polycrystalline nature of the coating with a hexagonal lattice of wurtzite type. The coherence-area length determined by the Scherrer formula is of 11.8 nm.

У роботі продемонстровано синтезу плівок оксиду Цинку ZnO методом ВЧ-магнетронного розпорошення цинкової мішені на кремнійовій підкладинці з використанням буферних шарів SiC та поруватого Si. Синтеза складалася з трьох етапів: одержання мезопоруватої поверхні Si(111) електрохемічним щавленням, нанесення плівок SiC на поруваті кремні-

йові підкладинки методом заміщення та синтези плівок ZnO за допомогою високочастотного магнетронного напорошення. Товщина плівки оксиду Цинку становила ≅ 1 мкм. Мікроскопічний розріз плівки ZnO демонструє її стовпчасту мікроструктуру. Плівки мають форму щільно пакованих (аґломерованих) нанозерен (розміром у 100–150 нм). За результатами рентґенофазових мірянь плівки ZnO орієнтовані уздовж основного напрямку текстури [0001]. Вивчення властивостей поверхні утвореної структури свідчить про полікристалічний характер покриття з гексагональною ґратницею типу вюрциту. Довжина области когерентности, визначена за Шерреровою формулою, становить 11,8 нм.

Key words: high-frequency magnetron sputtering, ZnO film, buffer layer, SiC film, mesoporous Si.

Ключові слова: високочастотне магнетронне розпорошення, плівка ZnO, буферний шар, плівка SiC, мезопористий Si.

(Received 18 January, 2022)

1. INTRODUCTION

Metal oxides (TiO_2, ZnO, Al_2O_3, Fe_2O_3, *etc.*) are very promising for many applications in micro- and optoelectronics. Among the above metal oxides, ZnO stands out due to its advantages: stability, good electronic conductivity, high chemical resistance, wide bandgap (3.1–3.3 eV), *etc.* [1, 2].

The manufactured electronic devices properties based on zinc oxide depend largely on the substrates. Recently, active researches conducted on the manufacture, properties and application of ZnO/Si heterostructures [3–5]. However, if zinc oxide films grown on silicon substrates, there is a problem associated with a significant difference in the lattice constants of these materials. This problem leads to the dislocations appearance in the structure. Concentrations of such penetrating dislocations can lead to significant deterioration of devices based on these heterostructures. To reduce the defects number in the SiC/Si heterostructure, the use of buffer layers is proposed [6–7]. In addition, buffer layers protect the Si substrate from chemical interaction with oxygen, water vapour, and chlorine-containing compounds [8] and prevent the appearance of amorphous and polycrystalline phases Zn_2SiO_4, $ZnSiO_3$, Zn, SiO_2 on the semiconductor interface [9]. One of the options is to use a SiC film as a buffer layer [10].

In this regard, further studies of the ZnO/Si system formation with an intermediate SiC layer and its effect on the surface properties of the obtained heterostructure are relevant.

The purpose of this article is to obtain ZnO/SiC/porous-Si/Si heterostructures, as well as to characterize the fabricated structures

surface comprehensively.

2. EXPERIMENTAL TECHNIQUE

The ZnO/SiC/porous-Si/Si heterostructure was obtained in several stages:

1. obtaining a mesoporous Si(111) surface by electrochemical etching;
2. deposition of SiC films on porous silicon substrates by the substitution method;
3. synthesis of ZnO films by high-frequency magnetron sputtering.

At the first stage, single-crystal Si(111) wafers of the *p*-type conductivity orientation were subjected to anodic etching in HF hydrofluoric acid solution HF. The samples were etched according to the standard technique [11].

At the next stage, silicon carbide layers were formed on mesoporous Si samples by atom substitution, according to the technique introduced in the works [12–14]. For this purpose, the samples, according to the Kukushkin–Osipov method [12], were annealed in an atmosphere of carbon monoxide (CO) and silane (SiH_4) gases mixture. A SiC growth process detailed description and the experimental setup scheme are presented in the review [13], the synthesis conditions are given in research [15].

The final stage was the ZnO thin films deposition by HF discharge of a zinc target in argon with oxygen [16]. Target parameters: diameter of 80 mm, thickness of 6 mm, zinc purity of 5N. Target–substrate distance is of 70 mm. Before deposition, the target was pre-sprayed for 10 minutes to remove all contamination. The samples were divided into two groups depending on the conditions of the deposition process (Table 1).

At the end of each stage, the test samples were thoroughly cleaned and degreased.

All experimental samples were examined by scanning electron and atomic force microscopy and x-ray microanalysis. The interface structure and the surface structure of the layers were studied using

TABLE 1. The conditions of synthesis of ZnO.

Parameter	Value
Growth time, second	600
Substrate temperature, °C	300
The residual pressure in the chamber, Pa	10^{-3}
Argon pressure, Pa	1
Oxygen pressure p_{O_2}, Pa	0.1
HF magnetron discharge power, W	200

a scanning electron microscope Tescan Mira 3 LMU, an atomic force microscope, and an Oxford Instruments X-Max 80 mm^2 energy dispersive spectrometer. X-ray structural studies were performed on a Panalytical X'Pert PRO MRD diffractometer using CuK_α radiation ($\lambda = 0.15406$ nm). Both x-ray phase analysis (XRD) and high-resolution diffractometric (HRXRD) methods were used for the study. A typical fast electron diffraction pattern (electronogram) from the surface (111) of SiC/Si films in the [110] direction was measured using an EPM-100 electronograph at an electron energy of 50 keV.

3. RESULTS AND DISCUSSION

According to the results obtained using scanning microscopy, after electrochemical etching, the initial Si surface of the orientation (111) underwent changes, *i.e.*, pores with a shape close to cylindrical were located at an angle to the Si surface. The pore diameter was of about 20 nm and the depth of the porous layer was of $\cong 1.5$ μm.

SEM images of the surface and end cuts of SiC/porous-Si samples (Fig. 1, *a*, *b*) demonstrate a significant change in the surface morphology after synthesis. A structure of small crystallites is observed

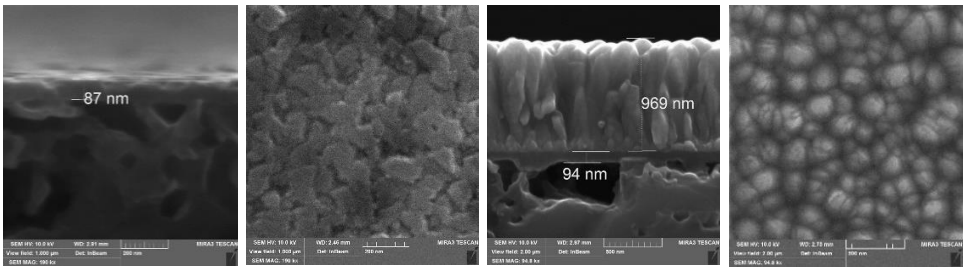

a *b* *c* *d*

Fig. 1. The SEM-image of a surface and cross-section: *a*, *b*—SiC films synthesized on mesoporous Si substrates; *c*, *d*—ZnO films.

TABLE 2. Elemental composition of the surface of the ZnO/SiC/porous-Si/Si.

Element	Percentage, %
Si	11.88
C	30.52
Zn	28.73
O	28.88

on the surface. Crystallites having an irregular spherical shape are with characteristic sizes at about tens to hundreds of nanometres. The cross-sectional image confirms the results obtained earlier by us in [17]. The SiC film covers the Si substrate, the porous structure is destroyed, and the volume of voids in the substrate is much larger than that usually observed during growth by atom substitution method [12–14].

After HF magnetron sputtering of the zinc target, the samples surface is covered with a continuous film. SEM images of the sample surface (Fig. 1, *c*, *d*) demonstrate a columnar film structure, which is ZnO films' characteristic. The high packing density leads to crystal splicing, which makes the film surface almost smooth and homogeneous, the maximum height of the profile irregularity being of 187.6 nm. This fact indicates the crystallites splicing and, consequently, the growing film thickening. The ZnO film on all samples is closely related to the SiC/porous-Si/Si substrate. There is no gap in the film/substrate interface.

X-ray fluorescence analysis was performed on the ZnO film surface (Table 2). The EDX spectra show lines of elements in both the substrate and the film. This is explained by the fact that, during microanalysis, the electron beam penetrates to a depth exceeding the thickness of the ZnO films.

Within the $2\theta/\omega$-scans obtained in the HRXRD mode near the reflection (111) of the Si substrate (Fig. 3), an asymmetry of this reflex is observed, which indicates the compression deformations presence in the substrate.

The diffraction peak in the region of the 35.58° angle corresponds

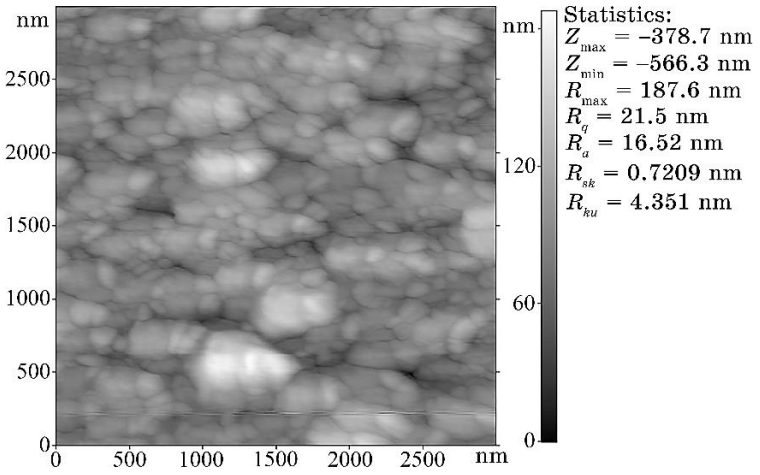

Fig. 2. The AFM-image of the surface of the ZnO/SiC/porous-Si/Si heterostructure.

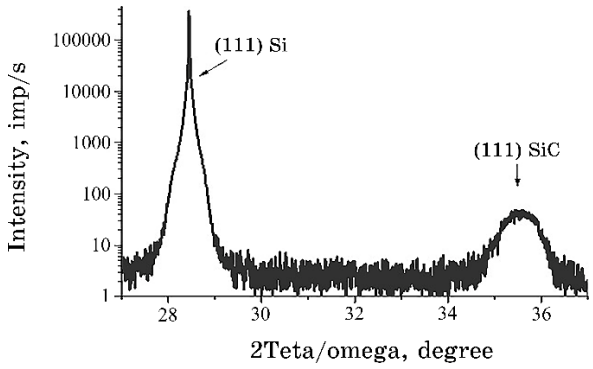

Fig. 3. 2θ/ω scanning reflex (111) from Si and SiC.

to the reflex (111) from the SiC film. The large broadening of this reflex is most likely caused by microstresses due to a significant mismatch of Si/SiC parameters. The diffraction peak blurring is most likely due to the fact that x-rays penetrate through the entire structure, including the broken boundary between SiC and Si. The root-mean-square deformation of the lattice (ε) in such a structure can be calculated by the formula [18]:

$$\varepsilon = \beta/4\mathrm{tg}\Theta, \qquad (1)$$

where β is the FWHM of the peak (002) (in radians), and θ is the diffraction angle (in radians). The average value estimate of the oscillation of the lattice parameter value perpendicular to the fusion plane calculated by the Eq. (1) is $\varepsilon = 1 \cdot 10^{-2}$.

Figure 4 shows a typical fast electrons diffraction pattern (electronogram) from the surface (111) of SiC/Si films in the direction [110]. The point reflexes of this electronogram clearly indicate that the Si surface contains a SiC epitaxial layer of the 3C–SiC polytype with the plane (111) extending to the substrate surface. The electronogram also shows that the SiC films are epitaxial, smooth, and contain no twins on the surface. The x-ray affects the entire structure and the broken SiC–Si boundary; so, it is blurred and the film itself is epitaxial.

The surface diffraction patterns of the ZnO/SiC/porous-Si/Si structure obtained by x-ray phase analysis (Fig. 5) have a classic triplet (100), (002), (101) of the hexagonal ZnO phase with parameters $a = 3.253$ Å, $c = 5.207$ Å.

The intensity of reflex (002) exceeds its value for reflex (101), indicating texture in the *c*-axis direction. The length of the coherence region determined by the Scherrer formula is of 11.8 nm. The diffraction patterns also show peaks of polycrystalline cubic SiC. In

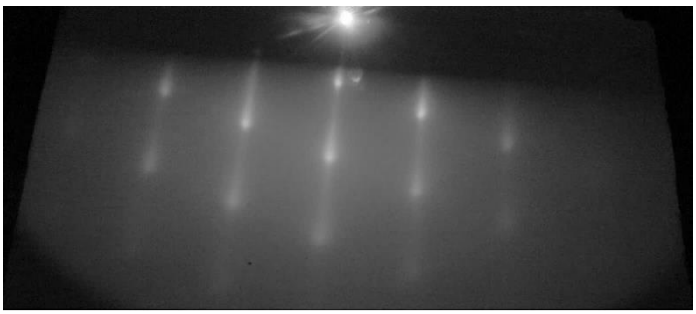

Fig. 4. Electron diffraction patterns from the surface of the SiC layer synthesized on the Si(111) surface with a preliminarily deposited mesopore system.

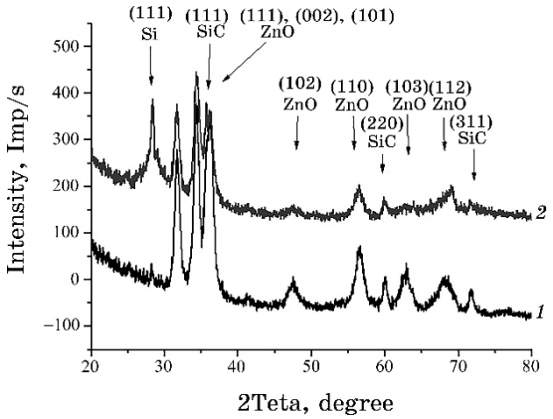

Fig. 5. Diffraction patterns of the x-ray phase analysis: curve *1*—the symmetric geometry of the survey $2\theta/\omega$, curve *2*—the diffractogram taken in the sliding geometry mode 2θ at the angle of incidence of the x-ray beam $\omega = 1°$.

the diffraction pattern taken in the sliding geometry (the incidence angle on the sample is 1°) at the position $2\theta = 28.44°$, we observe the (111) silicon reflex, although it is practically absent in the symmetric diffractogram $2\theta/\omega$. This effect can be explained by the presence of a thin polycrystalline Si layer at the Si/SiC interface, since sliding geometry is sensitive to thin near-surface layers.

4. CONCLUSION

The process of ZnO/SiC/porous-Si/Si/Si heterostructure formation was investigated during research. ZnO films were obtained by HF

magnetron sputtering on Si(111) substrates pre-profiled with mesopores using electrochemical etching, with a SiC buffer layer obtained by atom substitution. Using a set of methods of scanning electron and atomic force microscopy, x-ray spectral microanalysis and x-ray structural analysis, the morphology and structure of the ZnO film surface have been studied. The ZnO film surface properties study indicates the polycrystalline nature of the coating with a hexagonal lattice of the wurtzite type.

Thus, the SiC buffer layer makes it possible to obtain ZnO layers on silicon substrates, orients them, and protects the Si substrate from interaction with chemical elements during growth. This method of growing ZnO layers on Si substrate opens up new possibilities for application and new ways of synthesizing this material.

REFERENCES

1. A. Janotti and C. G. Van de Walle, *Rep. Prog. Phys.*, **72**, No. 12: 126501 (2009); https://doi.org/10.1088/0034-4885/72/12/126501
2. A. B. Djurišić, A. M. C. Ng, and X. Y. Chen, *Prog. Quantum Electron.*, **34**, No. 4: 191 (2010); https://doi.org/10.1016/j.pquantelec.2010.04.001
3. L. Ci-Hui, C. Yu-Lin, L. Bi-Xia, Z. Jun-Jie, F. Zhu-Xi, P. Cong, and Y. Zhen, *Chinese Phys. Lett.*, **18**, No. 8: 1108 (2001); https://doi.org/10.1088/0256-307X/18/8/338
4. D. Das and L. Karmakar, *J. Alloys Compd.*, **824**: 153902 (2020); https://doi.org/10.1016/j.jallcom.2020.153902
5. L. Chabane, N. Zebbar, M. Trari, Y. H. Seba, and M. Kechouane, *Mater. Sci. Semicond. Process.*, **13**: 105971 (2021); https://doi.org/10.1016/j.mssp.2021.105971
6. C. Xiong, L. Chen, W. Du, J. Ma, J. Xiao, and X. Zhu, *Int. J. Mod. Phys. B*, **31**, Nos. 16–19: 1744076 (2017); https://doi.org/10.1142/S0217979217440763
7. M. Kolhep, C. Sun, J. Bläsing, B. Christian, and M. Zacharias, *J. Vac. Sci. Technol. A*, **39**, No. 3: 032401 (2021); https://doi.org/10.1116/6.0000793
8. S. A. Kukushkin, V. I. Nikolaev, A. V. Osipov, E. V. Osipova, A. I. Pechnikov, and N. A. Feoktistov, *Phys. Solid State*, **58**, No. 9: 1876 (2016); https://doi.org/10.1134/S1063783416090201
9. S. A. Kukushkin, A. V. Osipov, and A. I. Romanychev, *Phys. Solid State*, **58**, No. 7: 1448 (2016); https://doi.org/10.1134/S1063783416070246
10. T. Phan and G. S. Chung, *Trans. Electr. Electron. Mater.*, **12**, No. 3: 102 (2011); https://doi.org/10.4313/TEEM.2011.12.3.102
11. A. F. Dyadenchuk and V. V. Kidalov, *Otrymannya Poruvatykh Napivprovidnykiv Metodom Ehlektrokhimichnogo Travlennya* [Obtaining Porous Semiconductors by Electrochemical Etching] (Berdyansk: BSPU: 2017) (in Ukrainian).
12. S. A. Kukushkin and A. V. Osipov, *J. Appl. Phys.*, **113**, No. 2, 024909 (2013); https://doi.org/10.1063/1.4773343
13. S. A. Kukushkin, A. V. Osipov, and N. A. Feoktistov, *Phys. Solid State*, **56**,

No. 8: 1507 (2014); https://doi.org/10.1134/S1063783414080137
14. S. A. Kukushkin and A. V. Osipov, *Phys. B: Condens. Matter*, **512**: 26 (2017); https://doi.org/10.1016/j.physb.2017.02.018
15. V. V. Kidalov, S. A. Kukushkin, A. V. Osipov, A. V. Redkov, A. S. Grashchenko, I. P. Soshnikov, M. E. Boiko, M. D. Sharkov, and A. F. Dyadenchuk, *Mater. Phys. Mech.*, **36**: 39 (2018); https://doi.org/10.18720/MPM.3612018_4
16. V. Kidalov, A. Dyadenchuk, Y. Bacherikov, A. Zhuk, T. Gorbaniuk, I. Rogozin, and V. Kidalov, *Turk. J. Phys.*, **44**, No. 1: 57 (2020); https://doi.org/10.3906/fiz-1909-10
17. V. V. Kidalov, S. A. Kukushkin, A. V. Osipov, A. V. Redkov, A. S. Grashchenko, I. P. Soshnikov, and A. F. Dyadenchuk, *ECS J. Solid State Sci. Technol.*, **7**, No. 4: 158 (2018); https://doi.org/0.1149/2.0061804jss
18. B. Abdullah and D. Tahir, *J. Phys. Conf. Ser.*, **1317**, No. 1: 012052 (2019); https://doi.org/10.1088/1742-6596/1317/1/012052